HARDWARE SIMULATION OF PARTICLE IDENTIFICATION ALGORITHMS FOR SILICON DETECTORS

S-R. Ban[1], D.L. Balabanski[1,2], Y. Fujikawa[3], T. Furuno[4], T. Kawabata[4], K. Sakanashi[4], P.-A. Söderström[1], M. Cuciuc[1]

We describe a hardware simulation of a particle identification (PID) technique, offering a novel alternative to traditional E-ΔE detector telescope and time-of-flight methods. Our approach involves accurately replicating the original software algorithms and analyzing the raw digitized waveforms. This work serves as a preceding step toward the future development of a fully hardware-based solution for PID.

Keywords: digital signal processing, charged particle spectrometry, particle identification

1. Introduction

Digital signal processing (DSP) is a widely recognized technique in nuclear spectroscopy. By analyzing the shape and amplitude of the incoming signals, various algorithms can be implemented to extract valuable information for further data processing.

In the context of particle identification (PID) and the detection of charged particles, the most common techniques are Time of Flight (ToF) and the E-ΔE methods. In the E–ΔE method, PID relies on correlating the energy deposit in the thin detector (ΔE) with the total energy measured by the thick detector (E). However, this method cannot be used with low-energy particles incapable of penetrating the first layer. On the other hand, the ToF method determines PID by correlating the detection time with the energy of charged particles. Achieving high resolution and performance with ToF requires a sufficiently

[1] Extreme Light Infrastructure - Nuclear Physics (ELI-NP), Horia Hulubei National Institute for R&D in Physics and Nuclear Engineering (IFIN-HH), 077125 Bucharest - Magurele, Romania

[2] Doctoral School in Engineering and Applications of Lasers and Accelerators, National University of Science R&D Technology POLITEHNICA Bucharest, 060042 Bucharest, Romania

[3]Department of Physics, Kyoto University, Sakyo, Kyoto 606-8502, Japan

[4]Department of Physics, Osaka University, Toyonaka, Osaka 560-0043, Japan

* corresponding author: e-mail: sara.ban@eli-np.ro

long flight path. Extending the flight path reduces the solid angle covered by detectors, diminishing detection efficiency, particularly in experiments involving multiple decay particles.

This article presents a hardware simulation of previously implemented work [1], adapted to meet hardware-based specifications.

2. Physics case: Motivation for the development

While the methods outlined in this paper are general and applicable to several possible experiments involving charged-particle emission, the specific case that motivated this work was an experiment on the radiative decay of the Hoyle state, performed at the 9MV Tandem accelerator of IFIN-HH [2] in 2022.

The Hoyle state is an excited state with spin-parity $J^\pi = 0^+$ in the ^{12}C nucleus, playing an essential role in the production of carbon during stellar nucleosynthesis. It is a cluster state consisting of three α-particles, with a total decay width Γ that mainly involves breakup back into three α particles. However, being a 0^+ state, it can also decay via electron conversion to the ground state, $\Gamma_\pi(E0)$, and radiatively by γ-ray emission to the first excited state, Γ_{rad}. While measuring these decay channels individually is challenging, the decay ratios can be determined, as discussed by Kibédi *et al.*[3].

$$\Gamma_{\text{rad}} = \left[\frac{\Gamma_{\text{rad}}}{\Gamma}\right]\left[\frac{\Gamma}{\Gamma_\pi(E0)}\right][\Gamma_\pi(E0)] \tag{1}$$

This state has an excitation energy level of 7.65 MeV, and its population typically occurs in two steps during stellar burning: first, helium fusion to the unstable ^{8}Be, which then captures a third helium nucleus to form ^{12}C. This process is illustrated in Fig. 1.

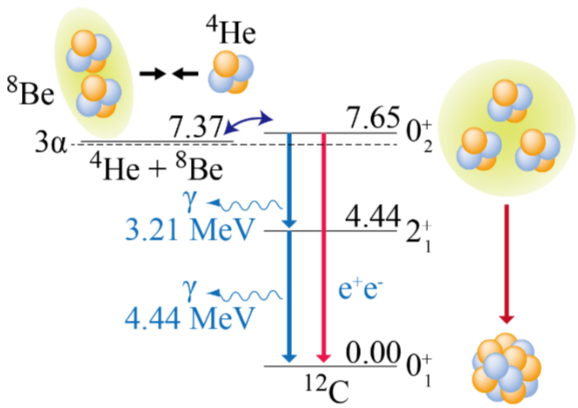

FIGURE 1. Schematic diagram of the 3-α reaction [4].

The 2022 experiment to measure the relative radiative branch of decay used an α-beam on a ^{12}C target aiming for triple-coincidence measurement of scattered/recoil particles and gamma rays. For this to be successful, effective particle identification methods are essential. In this case, offline pulse-shape analysis (PSA) techniques were chosen with the tradeoff of higher data acquisition software and hardware resource requirements in terms of data storage and processing time. With new open FPGA digitizers becoming more available, these drawbacks can be overcome by implementing PID methods in the electronic hardware for online processing.

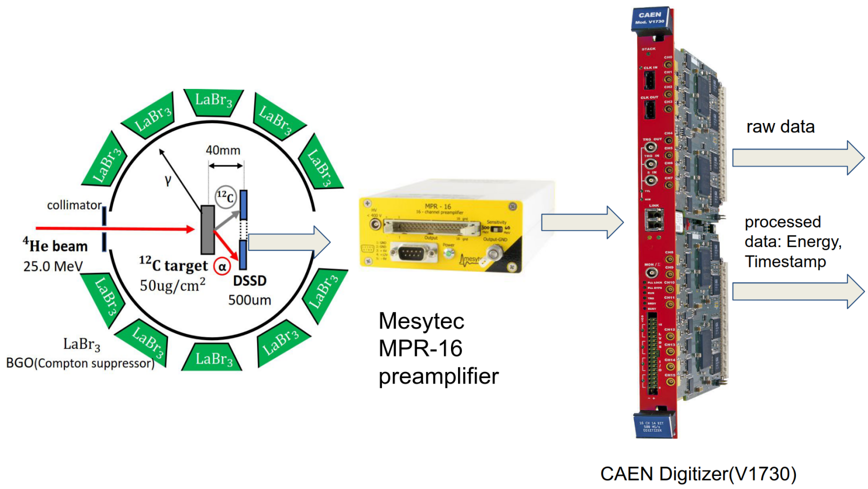

FIGURE 2. Schematic presentation of the experimental set-up for Measurement of the Radiative-Decay Probability of the Hoyle State experiment [1].

The experimental setup, depicted in Fig.2 consists of 24 $3'' \times 3''$ $LaBr_3$:Ce and $CeBr_3$ scintillation detectors placed in anti-Compton shields [5], involved extracting waveforms from a Double Sided Strip Detector (DSSD) using a Mesytec MPR-16 preamplifier connected to a CAEN V1730 digitizer [6]. The digitizer extracts pulse energy and timestamp by utilizing Pulse Height Analysis (PHA) [7]. Simultaneously, the raw signal waveforms were collected to apply a PSA algorithm, which will be detailed in the following section.

3. Algorithm

The PSA algorithm utilizes a triangle filter with two rolling averages applied to the incoming waveform, enabling the distinction of multiple incoming particles based on their rise times.

The output value y_n is calculated using the following equation for the triangle filter [8]:

$$y_n = \frac{1}{L}\left(\sum_{k=0}^{L-1} x_{n+k} - \sum_{k=-L}^{-1} x_{n+k}\right) \tag{2}$$

where y_n, x_n, and L denote the output value, the input value for each element n, and the length of the triangle filter, respectively. A parameter corresponding to the peak amplitude (A_{max}) of the processed signal was then extracted by computing the difference between the minimum and maximum values of the output values y_n.

4. Hardware simulation

The original implementation of the PSA algorithm was developed in ROOT/C++ [9] and described in K. Sakanashi's Master Thesis [10]. To facilitate deployment on a hardware platform, the objective of this project was to translate the code into Very High Speed Integrated Circuit Hardware Description Language (VHDL). The initial software version utilized floating-point arithmetic, but to align with the requirements of the hardware platform, the code was converted to use integer representation in preparation for future synthesis. The float-to-integer conversion was applied across all functional blocks of the design.

The block diagram consists of three main components: the baseline block, which calculates the baseline and performs the subtraction; the normalization block, which adjusts the signal to align with the integer representation; and the triangle filter block, which processes the waveforms as it is shown in Fig.3. Each block in the diagram represents a distinct function, which will be further explained in the following sections.

4.1. Blocks characteristics

The block diagram and VHDL code were developed using Xilinx Vivado 2022.2 toolchain. The incoming waveform is first fed into the baseline block, which is primarily responsible for calculating the baseline and determining the signal's maximum value. The normalization process adjusts the data such that it uses an integer representation. This ensures that when converting the data from a floating-point format to an integer format, it remains precise and fully uses the available resolution in subsequent hardware blocks.

The implementation of the triangle filter in the hardware simulation was accomplished using two First In, First Out (FIFO) blocks along with their respective accumulators, as shown in Fig.4 and described by Eq.(2). The depth of each FIFO is 16 entries, representing the window size for summing the elements.

For each trigger corresponding to an incoming particle, the A_{max} is calculated by a subsequent block by subtracting the minimum value from the maximum value of the triangle filter output for that waveform.

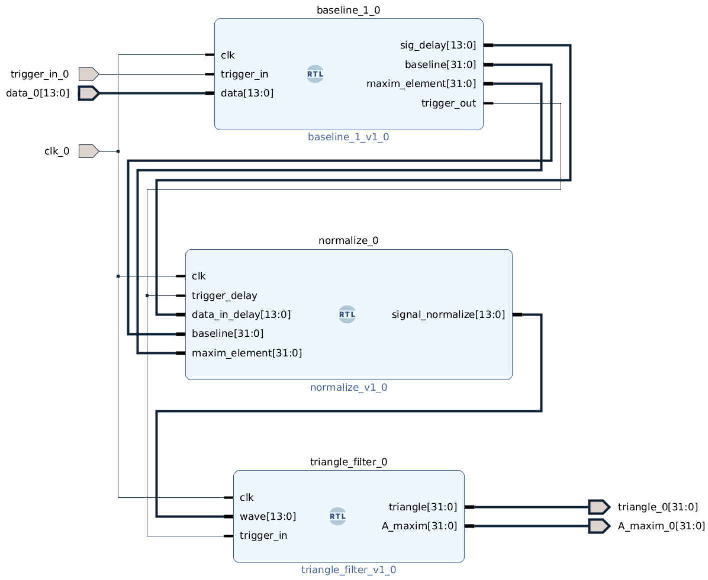

FIGURE 3. Xilinx Vivado design block diagram containing 3 main blocks: baseline computation, normalization, and triangle filter.

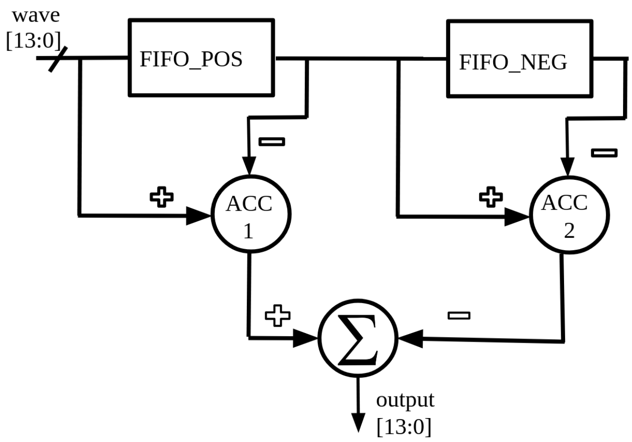

FIGURE 4. Hardware implementation of Eq.(2) for the triangle filter, consisting of two rolling averages realized using FIFO blocks and accumulators.

5. Results

The data was acquired using the CAEN V1730 digitizer, with each waveform sampled at a rate of 500MS/s. This resulted in waveforms comprising 800 samples, corresponding to a total data length of 1.6 µs as shown in Fig.5 (left).

The implementation of the algorithm can distinguish between different types of particles (α-particles, deuteron, and proton) by the differences in their respective waveforms' rise times. Figure 5 (right) shows the triangle filter output for each type of particle.

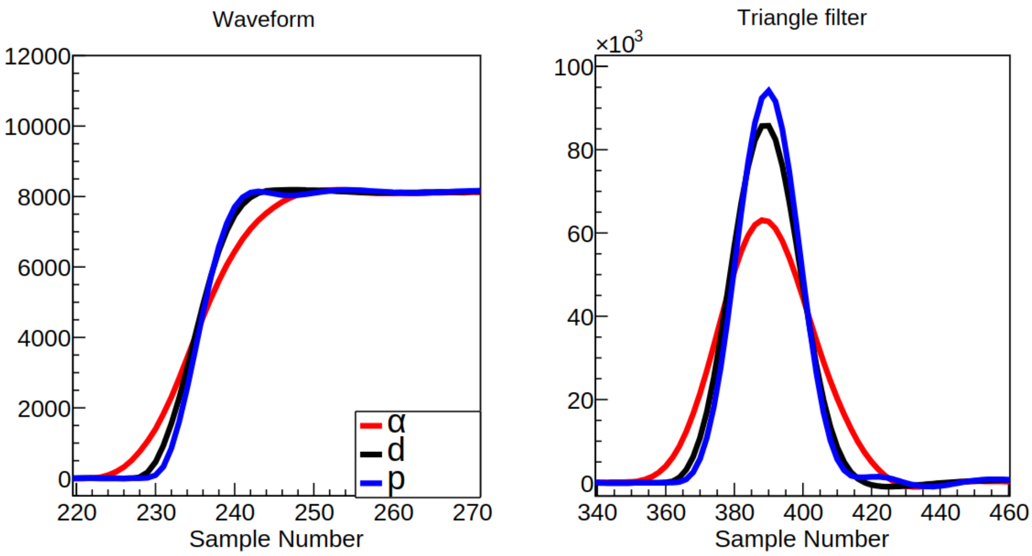

FIGURE 5. (Left) Raw waveform, and (right) output of the triangle filter. The rise time of each waveform varies depending on the type of incoming particle. α-particles, deuterons, and protons can be distinguished, serving as the basis for computing the A_{max} value.

A comparison between the software and the hardware simulation outputs was performed on a large dataset of waveforms. To better illustrate the correlation between the two results, a first-degree polynomial fit was applied. Residuals are plotted with respect to the linear fit. Points, where a substantial difference between the two algorithms can be observed, represent very low-amplitude waveforms where noise dominates the signal, as shown in Fig.6.

Figure 7 shows the particle identification performances of the two algorithms on the same data set: (a) uses the previous software-based work [8], [1], and (b) uses our hardware algorithm.

Distinct energy peaks at 9.64 MeV, 4.44 MeV, and the ground state are consistently observed in both algorithms. Additionally, the presence of ^{12}C is identifiable in both outputs.

We performed a Figure of Merit analysis (Eq.3) in the 12.5-13.5 MeV energy range (corresponding to ADC range of 7200–7800 in Fig. 7) to verify the efficiency of our algorithm. The distinction was made between α particles emitted from the target and those scattered from the beam by collimators. Due to their smaller incident angles, background α particles exhibited different signal characteristics, such as rise time, compared to those from the target.

$$\mathrm{FoM} = \frac{m_1 - m_2}{\mathrm{FWHM}_1 + \mathrm{FWHM}_2} \tag{3}$$

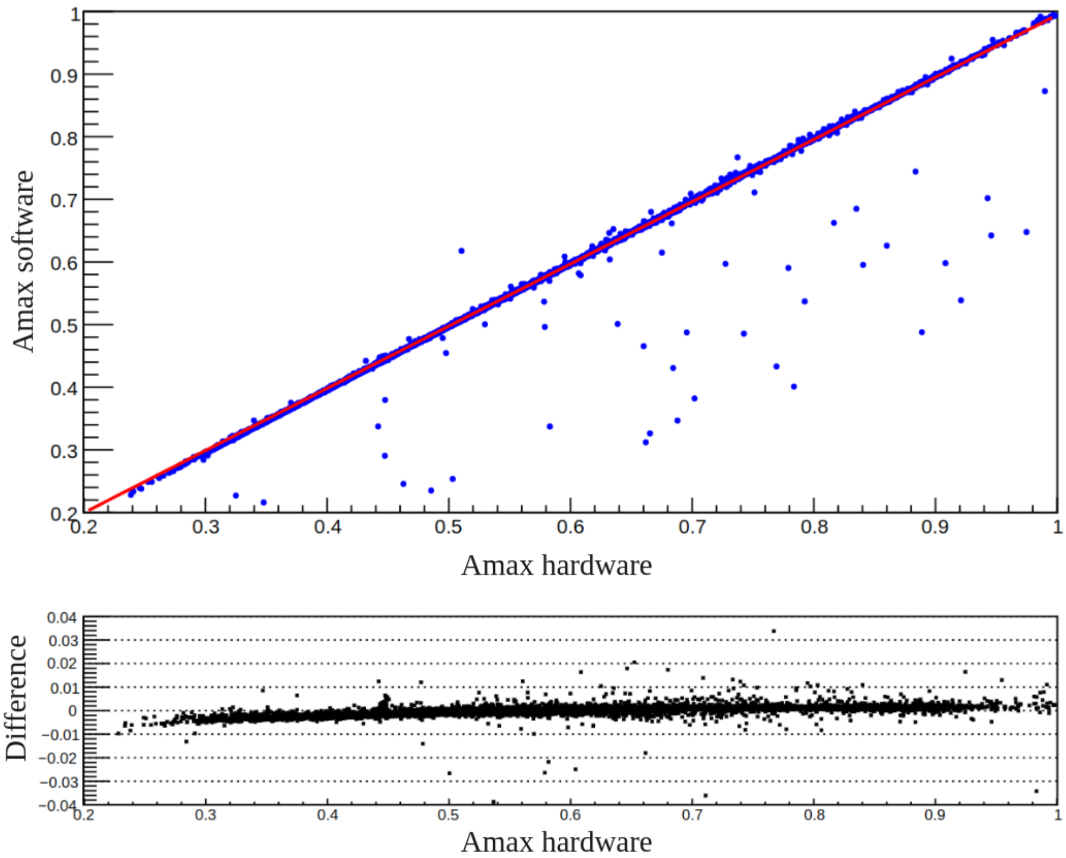

FIGURE 6. Comparison of software and hardware algorithm performance (top). Differences in software and hardware implementations (bottom). The red line indicates the first-degree polynomial fit.

The FoM was calculated based on the projection of the 12.5-13.5 MeV energy range on the A_{max} axis. The centroids of the peaks corresponding to α particles from the target (9.64 MeV) and those scattered by the collimator at a different angle are represented by m_1 and m_2. Similarly, $FWHM_1$ and $FWHM_2$ denote the full widths at half the maximum of these respective peaks.

Our algorithm achieved a FoM of 0.64$\pm$ 0.055, compared to 0.645$\pm$ 0.026 obtained using the software-based computation. This difference arises from the conversion of floating-point operations to integer arithmetic, a necessary step to facilitate hardware implementation.

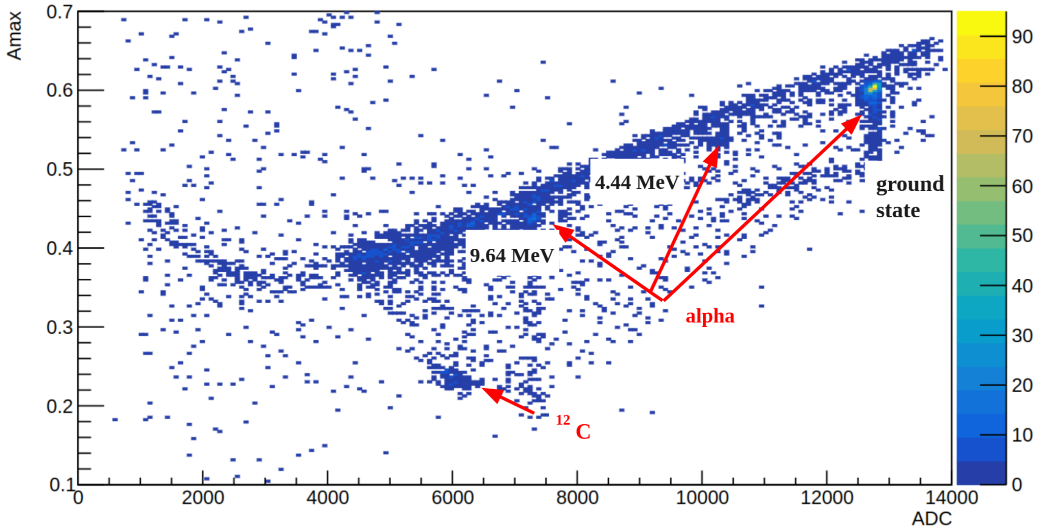

(a)

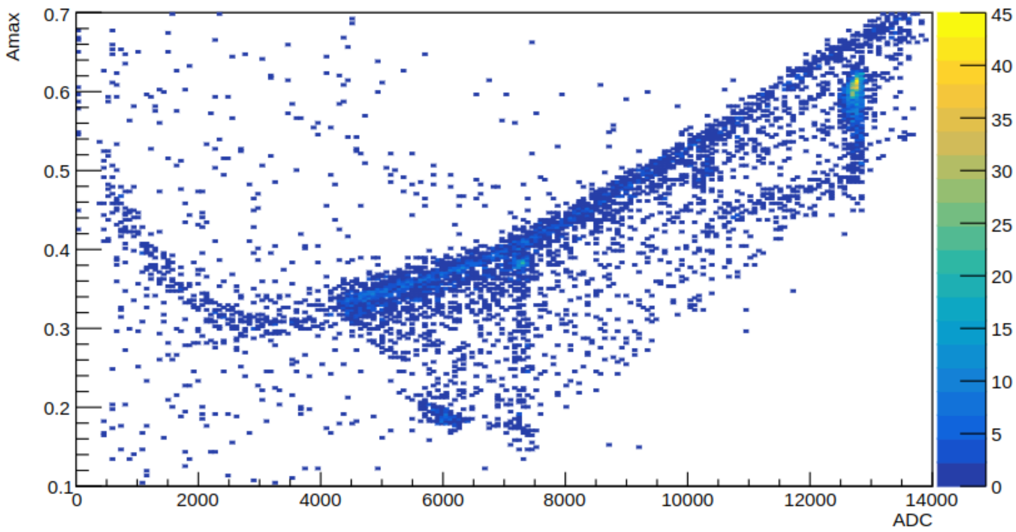

(b)

FIGURE 7. The comparison between the A_{max} values of the hardware (a) and software (b). In both cases, the energies from α are clearly visible, along with the presence of ^{12}C.

6. Conclusions and outlook

The algorithms discussed in this article have been successfully implemented in Xilinx Vivado using a hardware-based approach. The simulation results were compared with previous studies, and A_{max} showed similar outcomes as the software output. The next phase of the project involves real-time implementation and analysis on physical hardware, which is expected to enhance data processing speeds and overall system efficiency.

Acknowledgements

This work was supported under a contract funded by the Extreme Light Infrastructure Nuclear Physics Phase IV (PN23 21 01 06 Faza 4, Partea II) and by the Romanian Government through the National Programme "Installations and Strategic Objectives of National Interest". We acknowledge the support provided by the ELI-RO-RDI-2024-007 and ELI-RO-RDI-2024-002 projects, sponsored by the Romanian Ministry of Research, Innovation, and Digitalization.

REFERENCES

[1] Sakanashi Kosuke *et al.* Measurement of the radiative-decay probability of the hoyle state. *EPJ Web Conf.*, 306:01047, 2024.
[2] IFIN-HH 9 MV FN Pelletron Tandem Accelerator.
[3] T. Kibédi and Alshahrani *et al.* Radiative width of the hoyle state from γ-ray spectroscopy. *Phys. Rev. Lett.*, 125:182701, Oct 2020.
[4] Seiya Tsuji. Measurement of the electromagnetic decay probability of hoyle states using α inelastic scattering. Master's thesis, Department of Physics, Osaka University, 2022. Master's Thesis.
[5] S. Aogaki and D.L. Balabanski *et al.* A setup for high-energy -ray spectroscopy with the eli-np large-volume labr3:ce and cebr3 detectors at the 9 mv tandem accelerator at ifin-hh. *Nuclear Instruments and Methods in Physics Research Section A: Accelerators, Spectrometers, Detectors and Associated Equipment*, 1056:168628, 2023.
[6] CAEN. v1730, 2021.
[7] Valentin T. Jordanov and Glenn F. Knoll. Digital synthesis of pulse shapes in real time for high resolution radiation spectroscopy. *Nuclear Instruments and Methods in Physics Research Section A: Accelerators, Spectrometers, Detectors and Associated Equipment*, 345(2):337–345, 1994.

[8] Y. Fujikawa *et al.* Search for the 6 condensed state in 24mg using the 12c+12c scattering. *Physics Letters B*, 848:138384, 2024.

[9] Rene Brun and Fons Rademakers. Root - an object oriented data analysis framework. In *AIHENP'96 Workshop, Lausane*, volume 389, pages 81–86, 1996.

[10] K. Sakanashi. Using large-area si semiconductor detectors development of waveform discrimination techniques for low-energy charged particles. Master's thesis, Osaka University, 2021.